Dedicated to Prof. Edith A. Turi in recognition of her leadership in education

THE THERMAL DEGRADATION MECHANISM AND THERMAL MECHANICAL PROPERTIES OF TWO HIGH PERFORMANCE HETEROCYCLIC POLYMER FIBERS

Z. Wu[1], F. Li[1], L. Huang[2], Y. Shi[2], X. Jin[2], S. Fang[1], K. Chuang[3], R. E. Lyon[4], F. W. Harris[1] and S. Z. D. Cheng[1]*

[1]Maurice Morton Institute and Department of Polymer Science, The University of Akron, Akron, Ohio 44325-3909, USA
[2]Polymer Physics Laboratory, Center for Molecular Science, Institute of Chemistry, The Chinese Academy of Science, Beijing 100080, China
[3]NASA Lewis Research Center, Cleveland, Ohio 44135-3191
[4]Advanced Fire Resistant Materials, Fire Research Branch, Federal Aviation Administration Atlantic City International Airport, New Jersey 08405, USA

Abstract

The thermal mechanical properties and degradation behaviors were studied on fibers prepared from two high-performance, heterocyclic polymers, poly(*p*-phenylenebenzobisthiazole) (PBZT) and poly(*p*-phenylenebenzobisoxazole) (PBZO). Our research demonstrated that these two fibers exhibited excellent mechanical properties and outstanding thermal and thermo-oxidative stability. Their long-term mechanical tensile performance at high temperatures was found to be critically associated with the stability of the C–O or C–S linkage at the heterocyclic rings on these polymers' backbones. PBZO fibers with the C–O linkages displayed substantially higher thermal stability compared to PBZT containing C–S linkages. High resolution pyrolysis-gas chromatography/mass spectrometry provided the information of the pyrolyzates' compositions and distributions as well as their relationships with the structures of PBZT and PBZO. Based on the analysis of the compositions and distributions of all pyrolyzates at different temperatures, it was found that the thermal degradation mechanisms for both of these heterocyclic polymers were identical. Kevlar®-49 fibers were also studied under the same experimental conditions in order to make a comparison of thermo-oxidative stability and long-term mechanical performance at high temperatures with PBZO and PBZT fibers. The data of two high-performance aromatic polyimide fibers were also included as references.

Keywords: heterocyclic polymers, mechanical properties, thermal degradation

Introduction

The successful development of high-performance, heterocyclic polymeric fibers has been viewed as a classic example attesting to the importance of applying novel materials in a variety of application areas. The best known ones among this heterocyclic polymer

---

*   Author to whom all correspondence should be addressed.

family are poly(*p*-phenylenebenzobisthiazole) (PBZT) and poly(*p*-phenylene-benzobisoxazole) (PBZO). During the past two decades, extensive reports have appeared on their syntheses [1–3], lyotropic liquid crystalline phases [4, 5], fiber spinning and the fibers' mechanical properties [6–11], electric properties [6], and thermal stability [1–3].

In 1981, the thermal degradation of PBZT and PBZO in vacuum was studied using thermogravimetry-mass spectroscopy (TG-MS) [1, 2]. It was reported that at approximately 600°C, the heterocyclic rings started to be broken; at 1000°C, the total mass loss was approximately 28%. The degraded fragments were identified as H_2S, HCN, CS_2, CO, CO_2, etc. A detailed study of the thermal degradation and its mechanism is still awaited. In addition, one of the most important aspects of these materials' applications, the effect of thermal stability on their mechanical performance after a long-term aging, is not known. This property is particularly useful to consider in the manufacture of the containment of aircraft engines.

In this paper, we report our recent studies on the mechanical property changes under a long-term, high temperature aging and the thermal degradation mechanism of both high-performance PBZO and PBZT fibers. The Kevlar®-49 fiber is also investigated in this study. The thermal stability and mechanical performance in aging under the same experimental conditions for two high-performance aromatic polyimide fibers were reported previously [13–17] and they are used as reference data for comparison [18]. These two fibers were synthesized from 3,3',4,4'-biphenyl-tetracarboxylic dianhydride (BPDA) reacted with the diamine of 2,2'-bis(trifluoro-methyl)-4,4'-diaminobiphenyl (PFMB) and the other diamine of 2,2'-dimethyl-4,4'-diaminobiphenyl (DMB), abbreviated as BPDA-PFMB and BPDA-DMB fibers.

Experimental

Materials and fiber samples

The long-term stability of PBZO and PBZT fibers' mechanical property and their thermal degradation mechanisms were studied. These fibers were obtained from the Wright Airforce Laboratory and Dow Chemical Co. In order to evaluate these fibers' performance, the Kevlar®-49 fiber provided by DuPont Co. was also tested as a standard reference. The chemical structures of all these materials were
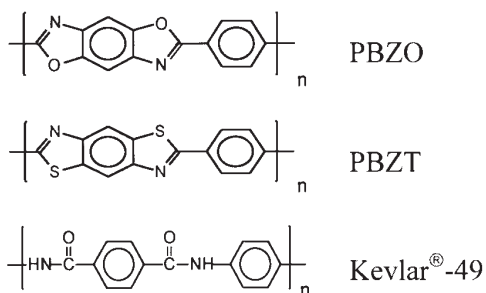
PBZO

PBZT

Kevlar®-49

Equipment and experiments

PBZO, PBZT, and Kevlar®-49 fibers were wound on a stainless steel frame. All fibers were isothermally aged in an air-circulating oven at 205°C under 1 atmosphere pressure for 100, 250, 500, 750, 1000, 1500, 2000, and 2500 h. The tensile strength, elongation to break, and initial modulus of each fiber were measured by using a Rheometrics RSA II, where a single filament was mounted on a gage with a length of 1.0 inch. The reported mechanical data were obtained by averaging 30 independent filament measurements. The typical standard deviation was around ±15%. All samples were elongated until they were broken at a constant rate of 6% per min.

Thermal gravimetry (TG) measurements were conducted in a TA TGA 2950. The isothermal mode was selected in order to determine the thermal degradation activation energy of those polymers. The temperature range was set to be 380–470°C. Mass losses were recorded *vs.* time at different isothermal heating temperatures. A typical sample mass of 3 mg was used.

High resolution pyrolysis-gas chromatography/mass spectrometry (HR Py-GC/MS) was used to study the thermal degradation mechanisms of PBZO and PBZT. The pyrolysis temperatures were set to be 764, 920 and 1040°C. Samples weighing from 0.3 to 0.5 mg were placed in a JHP-3 Curie Point Pyrolyzer (Japan Anal. Ind. Corp.). Each pyrolysis time was set to be 5 s. The separation and the identification of the fragments generated during thermal degradation were carried out through an on-line QP-5000 GC-MS (Shimadzu). The GC fused silica capillary column, CBP5 (0.25 mm i.d. $\times$25 m), was held at 50°C for 5 min, then temperature was programmed to 250°C at a heating rate of 5°C min^{-1}. The helium gas, with a total flow of 13 mL min^{-1} and a split ratio of 10:1, was used as the carrier gas. The electron impact source in the MS was operated at 70 eV and 250°C.

Results and discussion

Thermal degradation activation energies

Monitoring the mass change as a function of temperature is a commonly used TG measurement to determine materials' thermal stability. This kind of non-isothermal measurements under dry nitrogen or air atmospheres has been utilized in routine testing procedures. However, such kind of experiments provides limited information regarding to the thermal stability of materials. In principle, this type of observation seldom helps to elucidate any chemical reactions that occurred or to reveal the mechanism behind a thermal degradation. A more precise one, the isothermal heating TG measurements, can be performed to study the mass loss kinetics, which is directly related to the thermal stability of materials. Figures 1, 2 and 3 show the mass loss changes (in percentages) with time in the air at different isothermal temperatures for PBZO, PBZT, and Kevlar®-49 fibers, respectively. As shown in these figures, about a 3% mass loss of PBZO and PBZT fibers is detected at 400°C after 6.7 h. This indicates the excellent thermal stability of both PBZO and PBZT fibers. However, for the
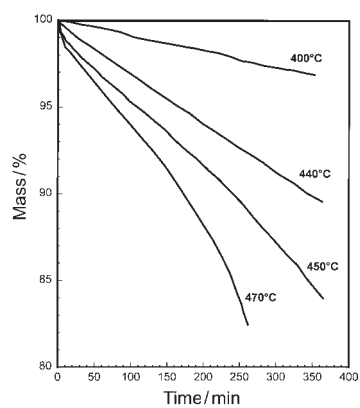
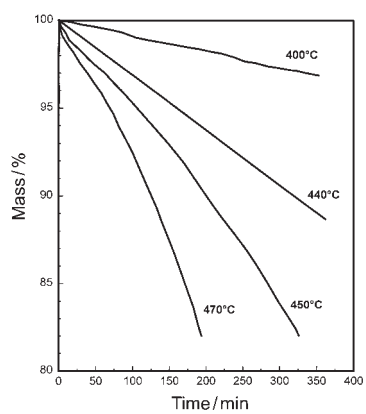**Fig. 1** Isothermal TG experiments for PBZO fibers in air at different temperatures

Fig. 2 Isothermal TG experiments for PBZT fibers in air at different temperatures
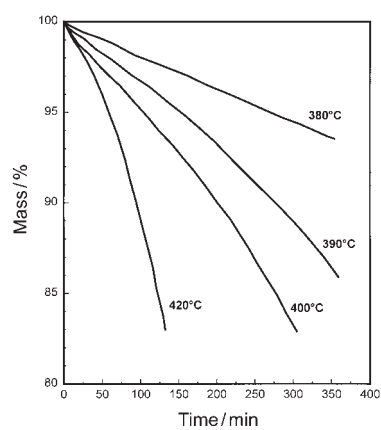

Fig. 3 Isothermal TG experiments for Kevlar fibers in air at different temperatures

Kevlar®-49 fiber, a mass loss of more than 20% is found under the same conditions. This difference verifies the possible thermo-oxidation occurred in the Kevlar®-49 fibers. Based on the kinetics model proposed by Flynn [19], mass loss activation energies of these fibers can be calculated using the following equation:

$$\ln(t) = \ln[g(\alpha)] - \ln A + E_a/(RT), \tag{1}$$

where t is the isothermal time; $g(\alpha)$ is the integral of the rate of mass loss; A is the pre-exponential factor; R is the gas constant; E_a is the mass loss activation energy. The slope of the plot of $\ln(t)$ *vs.* $1/T$ at constant mass fraction loss, $g(\alpha)$, yields E_a. The mass loss activation energies in air are calculated as 130, 115 and 100 kJ mol^{-1} for PBZO, PBZT, and Kevlar®-49 fibers, respectively. Compared to the previous data provided by our laboratory on two polyimide fibers, BPDA-PFMB and BPDA-DMB, these activation energies are lower. The two polyimide fibers possess the thermal degradation activation energies of 200 and 135 kJ mol^{-1} under the air atmosphere [18].

Changes of tensile properties during isothermal aging

The most reliable test on the thermal and thermo-oxidative stability of a fiber, in a practical sense, is the measurement of the particular mechanical (e.g., tensile) properties upon prolonged isothermal aging times at elevated temperatures. Figure 4 illustrates the tensile strength changes of PBZO, PBZT, and Kevlar®-49 fibers after aging at 205°C in circulating air at different observation times. The results from BPDA-PFMB and BPDA-DMB fibers are also included for comparison [18]. This figure shows that the PBZO fiber displayed the highest tensile strength (4.3 GPa), while the tensile strengths of other four fibers were comparable and in between 2.2–3 GPa. With the aging time increases, all of the tensile strengths decrease at different rates except for the BPDA-PFMB fiber case [18]. In order to clarify these different decreasing rates, each tensile strength retention *vs.* the aging time at 205°C is plotted in Fig. 5. It is evident that after 2500 h of aging, the tensile
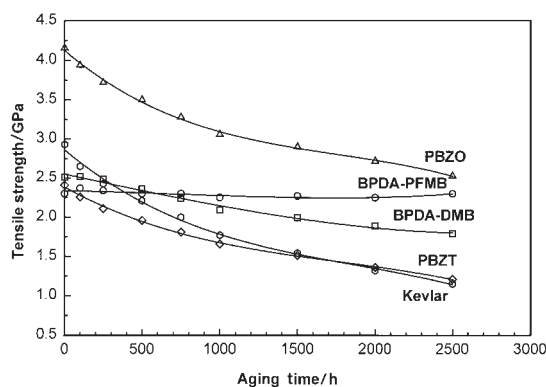

Fig. 4 Changes of the tensile strength of PBZO, PBZT and Kevlar fibers after aging at different intervals in circulating air at 205°C. The data of two aromatic polyimide fibers are also included for comparison
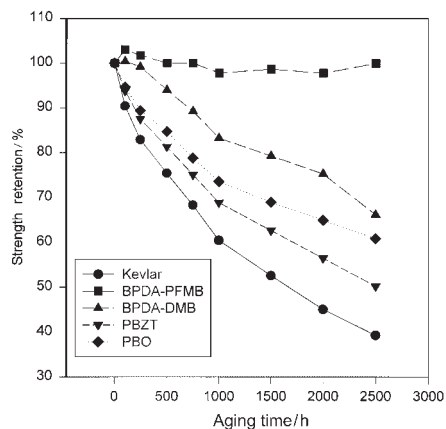
Fig. 5 Plot of percent strength retention of PBZO, PBZT and Kevlar fibers *vs.* isother-
mal aging time in circulating air at 205°C. The data of two aromatic polyimide
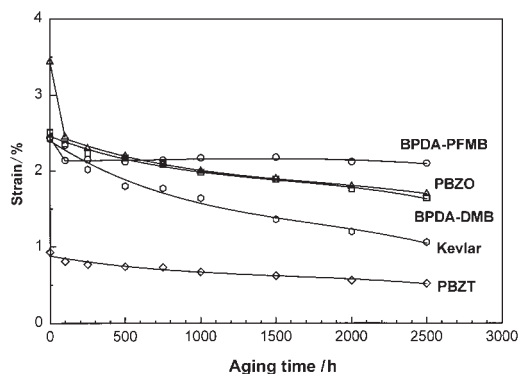fibers are also included for comparison

Fig. 6 Changes of the tensile strain of PBZO, PBZT and Kevlar fibers after aging at
different intervals in circulating air at 205°C. The data of two aromatic
polyimide fibers are also included for comparison

strength is retained almost 100% in the BPDA-PFMB fiber [18], about 70% in the
BPDA-DMB fiber [18], 60% in the PBZO fiber, 50% in the PBZT fiber, and 40% in the
Kevlar®-49 fiber.

As shown in Fig. 6, for the tensile strain change, the PBZO fiber shows an abnormal
decrease after 100 h. The strain decreases slightly in the PBZT fiber with the increase of
aging time, though its absolute value is below 1%; much lower (about 60% lower) than
that of other fibers. Both Kevlar®-49 and BPDA-DMB fibers exhibit gradual strain de-
creases, but the decreasing rate of the Kevlar®-49 fiber is faster than that of the
BPDA-DMB fiber. Moreover, the BPDA-PFMB fiber shows an almost constant strain,
after an initiate decrease of 0.2%. Again, in order to clarify the difference in these de-
creasing rates, each tensile strain retention *vs.* the aging time at 205°C is plotted in Fig. 7.
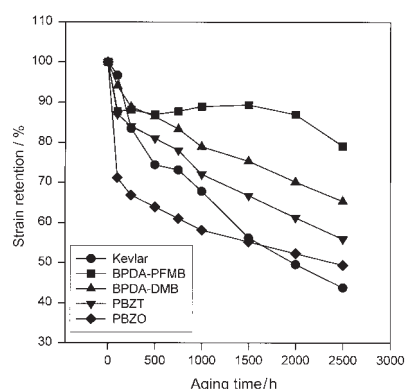In the PBZO fiber case, a 30% drop of strain is found after the first 100 h. After aging for

Fig. 7 Plot of percent strain retention of PBZO, PBZT and Kevlar fibers *vs.* isothermal aging time in circulating air at 205°C. The data of two aromatic polyimide fibers are also included for comparison

2500 h, the tensile strain retention of the PBZO fiber is about 52%. For the PBZT fiber after aging of 2500 h, the tensile strain retention reaches 58%; the Kevlar[®]-49 fiber shows a 55% loss in tensile strain. Compared with these fibers, both aromatic polyimide fibers display better performance. For the BPDA-PFMB fiber, the strain retention keeps almost constant after an initial 10% decrease, and the BPDA-DMB fiber maintains 68% of its tensile strain after aging for 2500 h [18].

During the isothermal aging in air, it is speculated that the changes of the macroscopic mechanical properties in a fiber, particularly of those tensile properties, may be due to the chemical structural changes induced by the scission of polymer chains, the completion of cyclization, and the crosslinking via chemical reactions. Secondary parameters, such as crystallization, crystal perfection, and orientation changes in a fiber may also affect those macroscopic properties. Nevertheless, during the isothermal aging in air, the changes of the macroscopic mechanical properties in a polymeric fiber is believed to originate mostly from the scission of the macromolecules as a result of thermal degradation.

Mechanism of decomposition

HR Py GC MS can provide useful information on the mechanism of the thermal degradation in polymers [20, 21]. In this study, PBZO and PBZT fibers are pyrolyzed under the same conditions in order to understand and compare their degradation mechanisms. The results of the PBZO and PBZT pyrolysis at 920°C obtained via high-resolution pyrolysis-total ion current chromatogram (HR Py-TIC) are shown in Figs 8 and 9. Major peaks on these chromatograms are assigned by using an on-line MS. The determined chemical structures of major pyrolyzates are listed in Table 1.

As shown in Figs 8 and 9, the pyrolyzates of PBZT and PBZO are classified into three categories. The first class consists of the low boiling point substances of CS_2, CO_2, HCN, and benzene, which are generated by the extensive scissions of polymeric chains.
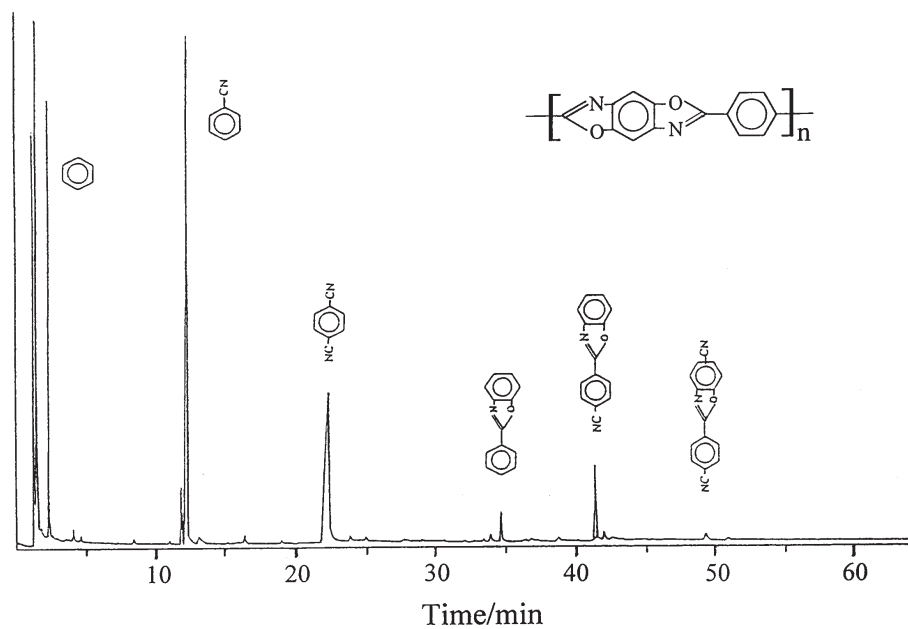
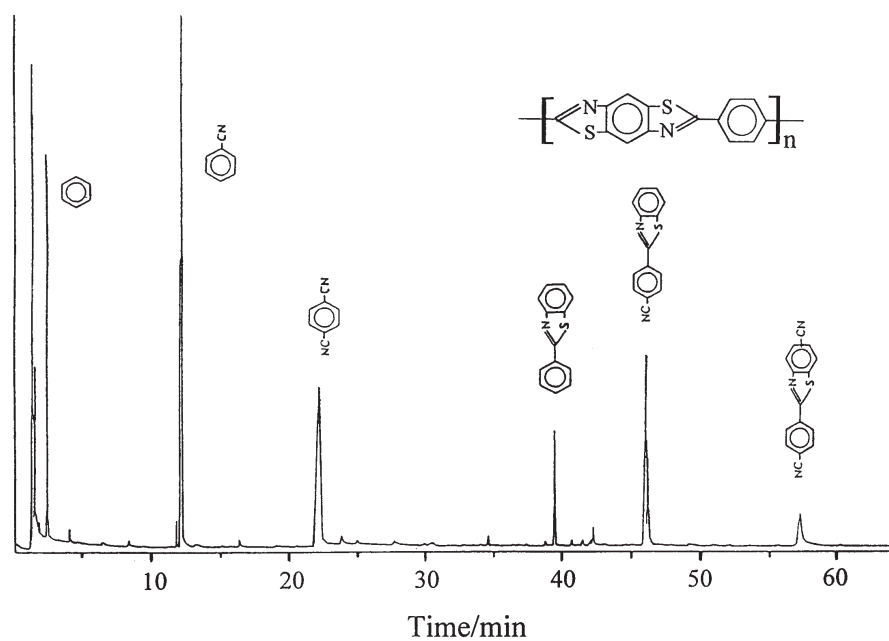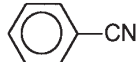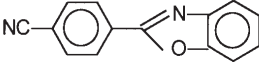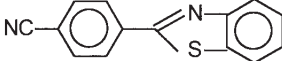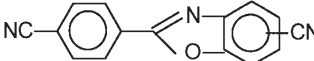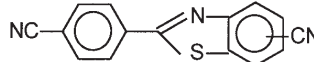**Fig. 8** High resolution TIC pyrogram of PBZO at a pyrolysis temperature of 920°C
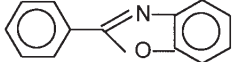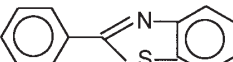
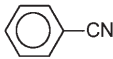**Fig. 9** High resolution TIC pyrogram of PBZT at a pyrolysis temperature of 920°C
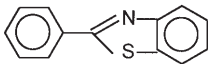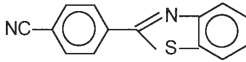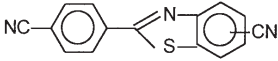
Table 1 The pyrolyzates of PBZO and PBZT fibers identified by PyGC/MS

No.	Structure	Name	MW	PBZO	PBZT
1		benzene	78	+	+
2		cyanobenzene	103	+	+
3		1,4-dicyano-benzene	128	+	+
4		2-phenyl benzoxazole	195	+	–
5		2-phenyl benzothiazole	211	–	+
6		2-(4-cyano-phenylene) benzoxazole	220	+	–
7		2-(4-cyano-phenylene) benzothiazole	236	–	+
8		2-(4-cyano-phenylene)-5-cyano-benzoxazole	245	+	–
9		2-(4-cyano-phenylene)-5-cyano-benzothiazole	261	–	+

+ observed, – not observed

The second class consists of cyanobenzene and 1,4-dicyanobenzene. For the C–N and C–S bonds located at the heterocyclic rings on both PBZO and PBZT backbones, their chemical bond energies are lower than that of a C–C bond. Pyrolysis is more likely to initiate at these heterocyclic rings because of the relatively lower thermal stability of C–O and C–S bonds. Consequently, the resulting pyrolyzates contain the characteristic –CN groups. The third class of pyrolyzates reflects the uniqueness of each heterocyclic ring on PBZO and PBZT backbones. The fragments of 2-phenyl benzothiazole (No. 5), 2-(4-cyanophenylene)benzothiazole (No. 7), and 2-(4-cyanophenylene)-5-cyano-benzothiazole (No. 9) are expected to originate from the PBZT pyrolysis. For the same reason, the PBZO pyrolysis gives rise to the fragments of 2-phenyl benzoxazole (No. 4), 2-(4-cyanophenylene) benzoxazole (No. 6), and 2-(4-cyanophenylene)-5-cyano-benzoxazole (No. 8). The formation of these fragments is also directly related to the cleavage of those heterocyclic rings, but these pyrolyzates' yields are lower than those of cyanobenzene and 1,4-dicyanobenzene.

Table 2 Pyrolyzate yields of PBZT fibers at different pyrolysis temperatures (calculated in peak area, %)

No.	Pyrolyzate Structure	Pyrolysis temperature/ 764°C	920°C	1040°C
1		31.4	19.0	24.2
2		40.4	39.5	46.2
3		12.8	23.2	19.9
5		4.6	5.8	1.3
7		10.9	12.4	8.3
9		–	–	–

Although the pyrolysis time is extended, only a few traces of pyrolyzates are detected from both the PBZO and PBZT fibers when the heating temperature is lower than 764°C. This justifies the pronounced thermal stability of PBZO and PBZT at high temperatures. Between 764 and 1040°C, the composition and the characteristics on chromatograms of PBZO and PBZT pyrolysis are almost the same. This implicates a similar mechanism behind the pyrolysis of both PBZO and PBZT in a wide temperature range. Tables 2 and 3 list the relative yields of various pyrolyzates from PBZO and PBZT *vs.* the pyrolysis temperatures, assuming that the total area integrated under all pyrolysis peaks is 100% on each chromatogram. Table 2 indicates that for PBZT, the yields of relatively longer chain fragments with heterocyclic structure (No. 5 and No. 7) increases when the heating temperature rises from 764 to 920°C. In this case, the yield of 1,4-dicyanobenzene also increases, whereas the yield of the low molecular mass pyrolyzate, i.e. benzene, decreases. This implies that the increment of pyrolysis temperature favors the growth of decomposing fragments with high molecular masses. On the other hand, ultra-high temperature (1040°C) leads to an increase in lower molecular mass yields (No. 1 and No. 2) but a decrease in high molecular mass yields (No. 5 and No. 7). This reduction is due to the fact that at extremely high temperature, the catastrophic thermal degradation would easily rip these polymeric molecules into smaller pieces. Comparing Table 2 with Table 3, a clear difference between the pyrolyzates' yields generated from PBZO and PBZT can be
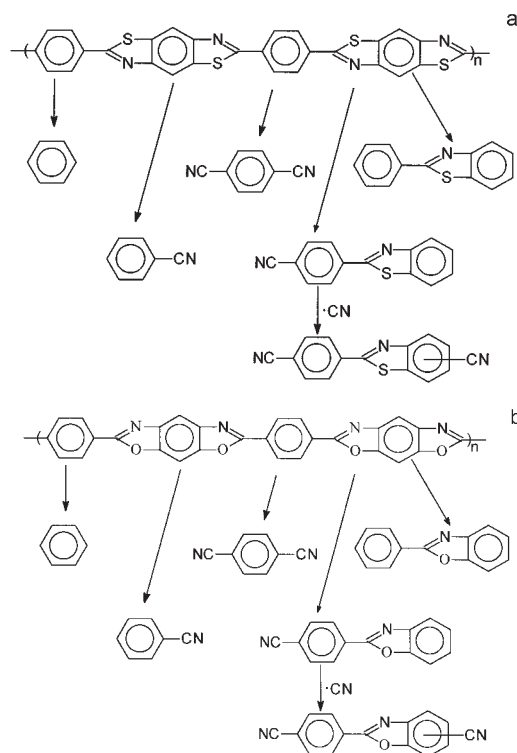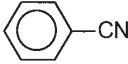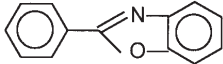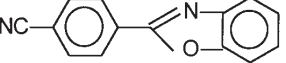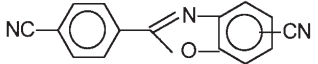
Fig. 10 Thermal degradation mechanism of PBZT (a) and PBZO (b)

ascertained, suggesting the distinctive heterocyclic ring structure on each polymer's backbone. Obviously, the growth of one 1,4-dicyanobenzene molecule involves the destruction of two C–N and two C–S bonds for PBZT but two C–N and C–O bonds for PBZO. Since the bond energy of the C–O bond is larger than that of the C–S bond, PBZO needs more energy than PBZT does in order to generate 1,4-dicyanobenzene. Furthermore, increasing temperature from 764 to 920°C has little effect on the yield of 1,4-dicyanobenzene from the PBZO pyrolysis, yet, under the same circumstance, this yield from PBZT greatly increases. However, when temperature is raised from 920 to 1040°C, 1,4-dicyanobenzene generated from both PBZT and PBZO decomposes further into cyanobenzene. Thus, the yield of 1,4-dicyanobenzene decreases, while the yield of cyanobenzene increases in both PBZT and PBZO cases. For the similar reason, between 764 and 1040°C, the yields of relatively high molecular pyrolyzates from the PBZO fibers, i.e. No. 4 and No. 6, are lower than the yields of No. 5 and No. 7 from the PBZT fibers. The exception is the comparison of the yields of No. 4 and No. 5 at 764°C.

The pyrolysis mechanisms of PBZT and PBZO are found to be identical, based on the assumption that the pyrolysis obeys the random initiation model and the analysis on the composition and distribution of the pyrolyzates generated from

Table 3 Pyrolyzate yields of PBZO fibers at different pyrolysis temperatures (calculated in peak area, %)

No.	Pyrolyzate Structure	Pyrolysis temperature/		
		764°C	920°C	1040°C
1		30.4	27.3	27.3
2		41.3	51.8	55.2
3		19.6	18.1	15.2
4		5.2	1.4	0.6
6		3.6	1.5	1.0
8		–	–	–

each material's pyrolysis. It is concluded that the pyrolysis starts either at the heterocyclic rings or at the C–C bond connected between the heterocyclic and benzene rings. As a result, cyanobenzene, 1,4-dicyanobenzene, and chain radicals containing heterocyclic and benzene rings are generated in a random pyrolysis fashion. Sequentially, combining with the hydrogen shift of C–H on aromatic rings, the depropagation reaction generates not only the fragments of cyanobenzene molecules, but also the fragments containing the characteristic heterocyclic and benzene rings. The pyrolysis mechanisms of PBZT and PBZO are shown in Fig. 10. The pyrolyzates identified and shown in this figure accord well with the molecular structures of PBZT and PBZO.

Conclusions

It is evident that both PBZO and PBZT fibers possess good thermal and thermo-oxidative stability. Their mass loss activation energies in air were determined using TG experiments. The long-term thermal aging testing indicates that these fibers exhibit reasonable mechanical property retention. In particular, the PBZO fiber is found to be thermally more stable, and it exhibits more retention of its mechanical tensile properties than the PBZT fiber does. Since PBZT contains the C–S bonds and PBZO possesses the C–O bonds on their backbones, while the

other parts of the chemical structures of these two polymers are identical, it is concluded that these two different bonds would substantially affect the thermal stability of these polymers. Based on the results of the compositions and distributions of those pyrolysis products, it is found that the thermal degradation of PBZO and PBZT fibers is based on the same mechanism.

* * *

References

1 J. F. Wolfe and F. E. Arnold, Macromolecules, 14 (1981) 909.
2 J. F. Wolfe, B. H. Loo and F. E. Arnold, Macromolecules, 14 (1981) 915.
3 F. E. Arnold, Jr. and F. E. Arnold, Adv. Polym. Sci., 117 (1994) 257.
4 A. W. Chow, J. F. Sandell and J. F. Wolfe, Polymer, 29 (1988) 1307.
5 A. W. Chow, R. D. Hamlin and C. M. Ylitalo, Macromolecules, 25 (1992) 7135.
6 H. Jiang, W. W. Adams and R. K. Eby, Fibers from Polybenzoxazoles and Polybenzothiazoles, Handbook of Fiber Science and Technology, Vol. III, Part D, Eds M. Lewin and J. Preston, 1996, pp. 171–246.
7 S. R. Allen and R. J. Farris, in The Materials Science and Engineering of Rigid Rod Polymer (W. W. Adams, R. K. Eby and D. E. McLemore Eds) 1989, p. 134.
8 S. R. Allen, A. G. Filippov, R. J. Farris and E. L. Thomas, Macromolecules, 14 (1981) 1135.
9 E. W. Choe and S. N. Kim, Macromolecules, 14 (1981) 920.
10 S. R. Allen, R. J. Farris and E. L. Thomas, J. Mater. Sci., 20 (1985) 2727.
11 S. R. Allen, A. G. Filippov, R. J. Farris and E. L. Thomas, J. Appl. Polym. Sci., 26 (1981) 291.
12 S. Z. D. Cheng, Z. Q. Wu, M. Eashoo, S. L. C. Hsu and F. W. Harris, Polymer, 32 (1991) 1803.
13 M. Eashoo, D. X. Shen, Z. Q. Wu, C. J. Lee, F. W. Harris and S. Z. D. Cheng, Polymer, 34 (1993) 3209.
14 M. Eashoo, D. X. Shen, Z. Q. Wu, F. W. Harris, S. Z. D. Cheng, K. H. Gardner and B. S. Hsiao, Macromol. Chem., 195 (1994) 2207.
15 D. X. Shen, Z. Q. Wu, J. Liu, L. Wang, S. Lee, F. W. Harris, S. Z. D. Cheng, J. Blackwell, T. Wu and S. Chvalun, Polymers & Polym. Composites, 2 (1994) 149.
16 W. Li, Z. Wu, H. Jiang, F. W. Harris and S. Z. D. Cheng, J. Mater. Sci., 31 (1996) 4423.
17 W. Li, Z. Wu, M. Leland, J. Y. Park, F. W. Harris and S. Z. D. Cheng, J. Macromol. Sci. Phys., B36 (1997) 315.
18 F. Li, L. Huang, Y. Shi, X. Jin, Z. Wu, Z. Shen, C. Chung, R. E. Lyon, F. W. Harris and S. Z. D. Cheng, J. Macromol. Sci. Phys., B38 (1999) 107.
19 J. H. Flynn, in Laboratory Preparation for Macromolecular Chemistry, E. McCaffrey Ed., McGraw Hill, New York 1970, p. 255.
20 Z. Jiang, X. Jin, X. Gao, W. Zhou, F. Lu and Y. Luo, J. Anal. Appl. Pyrolysis, 33 (1995) 231.
21 Y. Luo, R. Huo, X. Jin and F. E. Karasz, J. Anal. Appl. Pyrolysis, 34 (1995) 229.